

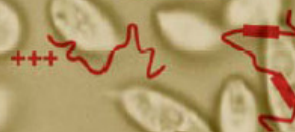
DE GRUYTER

2012 · VOLUME 393 · NUMBER 6
ISSN 1431-6730 · e-ISSN 1437-4315

BIOLOGICAL CHEMISTRY

BIOLOGICAL CHEMISTRY

2012 · VOLUME 393 · NUMBER 6 · PP. 429–XXX



EDITOR-IN-CHIEF
Bernhard Brüne



DE
G

www.degruyter.com/bc

DE GRUYTER

Mitochondrial protein import pathways are functionally conserved among eukaryotes despite compositional diversity of the import machineries

Elisabeth Eckers¹, Marek Cyrklaff¹, Larry Simpson² and Marcel Deponte^{1,2,*}

¹Department of Parasitology, Ruprecht-Karls University, Im Neuenheimer Feld 324, D-69120 Heidelberg, Germany

²Department of Microbiology, Immunology and Molecular Genetics, University of California Los Angeles, Los Angeles, CA 90095, USA

* Corresponding author
e-mail: marcel.deponte@gmx.de

Abstract

Mitochondrial protein import (MPI) is essential for the biogenesis of mitochondria in all eukaryotes. Current models of MPI are predominantly based on experiments with one group of eukaryotes, the opisthokonts. Although fascinating genome database-driven hypotheses on the evolution of the MPI machineries have been published, previous experimental research on non-opisthokonts usually focused on the analysis of single pathways or components in, for example, plants and parasites. In this study, we have established the kinetoplastid parasite *Leishmania tarentolae* as a model organism for the comprehensive analysis of non-opisthokont MPI into all four mitochondrial compartments. We found that opisthokont marker proteins are efficiently imported into isolated *L. tarentolae* mitochondria. *Vice versa*, *L. tarentolae* marker proteins of all compartments are also imported into mitochondria from yeast. The results are remarkable because only a few of the more than 25 classical components of the opisthokont MPI machineries are found in parasite genome databases. Our results demonstrate that different MPI pathways are functionally conserved among eukaryotes despite significant compositional differences of the MPI machineries. Moreover, our model system could lead to the identification of significantly altered or even novel MPI components in non-opisthokonts. Such differences might serve as starting points for drug development against parasitic protists.

Keywords: kinetoplastid parasites; *Leishmania tarentolae*; mitochondria; protein transport.

Introduction

Mitochondria are universal organelles of eukaryotes. They are involved in numerous cellular processes, such as

oxidative phosphorylation, lipid and amino acid metabolism as well as programmed cell death. According to current theories, the essentiality of these organelles is based on the importance of iron-sulphur cluster biosynthesis (Embley and Martin, 2006; Gross and Bhattacharya, 2009; Lill, 2009). As mitochondria are double membrane-bound organelles, they have four major compartments: the matrix, the inner membrane (IM), the intermembrane space (IMS) and the outer membrane (OM) (Neupert and Herrmann, 2007; Chacinska et al., 2009; Endo and Yamano, 2009). In the evolution of eukaryotes, most of the mitochondrial genes from the original eubacterial endosymbiont were either lost or transferred to the nuclear genome (Gross and Bhattacharya, 2009). Consequently, the majority of mitochondrial proteins are nuclear encoded, synthesised in the cytosol and imported into one of the four compartments following different MPI pathways and utilising different essential MPI machineries (Neupert and Herrmann, 2007; Chacinska et al., 2009; Endo and Yamano, 2009) (Figure 1). The current models of MPI are predominantly based on experiments with *Saccharomyces cerevisiae* and *Neurospora crassa*. Both organisms, together with metazoa, belong to the same group of eukaryotes, the opisthokonts (Adl et al., 2005; Cavalier-Smith, 2010) (Figure 1A). Consequently, several genome database-driven hypotheses on the functionality and evolution of the MPI machineries have been published (Dolezal et al., 2006; van Dooren et al., 2006; Allen et al., 2008; Schneider et al., 2008; Gross and Bhattacharya, 2009; Dolezal et al., 2010; Hewitt et al., 2011). However, so far, experimental (wet lab) research on non-opisthokonts has usually focused on the analysis of single MPI pathways or components in, for example, plants and parasitic protists including *Entamoeba* (Dolezal et al., 2010), kinetoplastid parasites (Hauser et al., 1996; Häusler et al., 1997; Gentle et al., 2007; Singha et al., 2008), *Blastocystis* (Tsaousis et al., 2011), *Trichomonas* and *Giardia* (Smid et al., 2008; Dagley et al., 2009; Hewitt et al., 2011).

Here, we present a comprehensive analysis of MPI in a non-opisthokont. To investigate the overall composition and function of MPI machineries in parasitic protists, we first performed exhaustive sequence analyses *in silico*. We then chose the kinetoplastid parasite *Leishmania tarentolae* as an experimental model system. To our knowledge, we established for the first time a parasitic protist for the analysis of non-opisthokont MPI into all mitochondrial compartments. Our data reveal that all known MPI pathways are functionally conserved among eukaryotes despite remarkable compositional diversity of the import machineries.

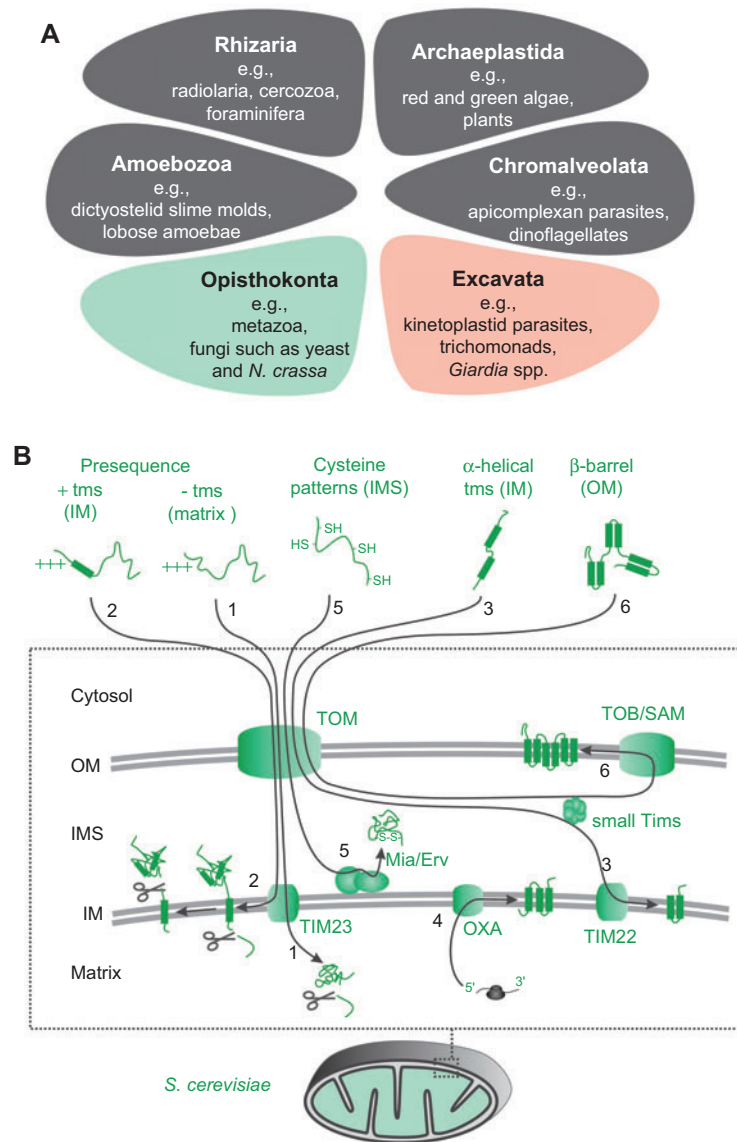


Figure 1 Current models of MPI pathways and machineries in opisthokonts.

(A) Opisthokonts represent just one of several major groups of eukaryotes (Adl et al., 2005). Metazoa as well as the model organisms *S. cerevisiae* and *N. crassa* belong to the opisthokonts, whereas parasitic protists (e.g., apicomplexan and kinetoplastid parasites) are found in different major groups of eukaryotes. (B) The current models of six different MPI pathways and machineries are based on studies with opisthokonts (Neupert and Herrmann, 2007; Chacinska et al., 2009; Endo and Yamano, 2009). tms, transmembrane segment.

Results and discussion

Identification of central and novel MPI machinery candidates *in silico*

Analysing parasite genome databases by BLAST, hidden Markov model and peptide motif searches, we found kinetoplastid homologues with a high sequence similarity to the opisthokont proteins Tob55/Sam50, Erv1, small Tims, Tim17 and Oxa1 (Figure 2A and Table 1). Additional candidates including Tom40, Tim22, Tim23 and Tim50 were identifiable in the genomes of apicomplexan parasites (Table 1). To facilitate future analyses in other eukaryotes, we also determined conserved peptide patterns of the identified proteins

by multiple sequence alignments. On the one hand, the motifs, which are summarised in Table 2, gave good results in reciprocal searches and suggest important functional and/or structural roles. On the other hand, many candidates, including the essential protein Mia40, as well as homologues of opisthokont receptor proteins with larger domains in the cytosol or IMS, shared very low sequence similarities or could not be identified at all. Our results mostly confirm previous *in silico* studies (Dolezal et al., 2006; van Dooren et al., 2006; Gentle et al., 2007; Allen et al., 2008; Schneider et al., 2008; Dagley et al., 2009; Gross and Bhattacharya, 2009; Hewitt et al., 2011), but additionally lead to the identification of putative homologues of novel small Tims, Tim50 and Tom40 (Tables 1 and 2, Figures S1 and S2 and Supplementary Results

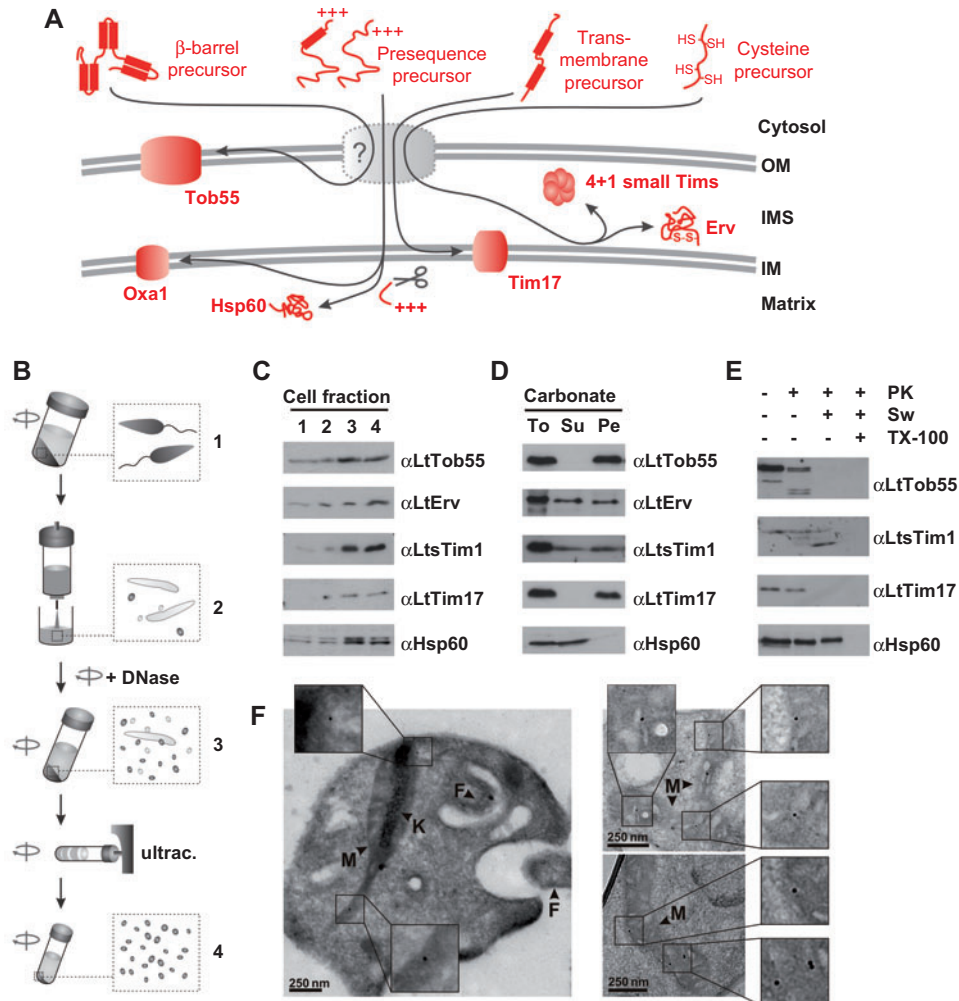


Figure 2 Establishment of mitochondrial markers in *L. tarentolae*.

(A) Identified MPI components in kinetoplastid parasite genomes. Please note that only few of the classical MPI components are found. For example, all components of the TOM and TIM22 complexes as well as the essential protein Mia40 seem to be absent. (B) Purification scheme for *L. tarentolae* mitochondria. Fraction 1, washed cells before lysis; fraction 2, whole cell lysate; fraction 3, crude mitochondrial preparation; fraction 4, final preparation. (C) Detection of *L. tarentolae* marker proteins in fractions 1–4 by Western blotting using the indicated peptide antibodies (Figure S3) and an antibody against conserved Hsp60 (positive control). (D) Protein solubility assays using carbonate treatment of isolated mitochondria. To, total protein; Su, supernatant; Pe, pellet. (E) Submitochondrial localisation studies using proteolytic susceptibility assays (see text). (F) Submitochondrial localisation studies of *LtErv* using immunogold electron microscopy. M, mitochondrion; K, kinetoplast; F, flagellum in flagellar pocket.

and Discussion 1). Noteworthy, we did not only identify a fourth small Tim candidate in kinetoplastid parasites that has been overlooked so far, but also discovered a novel class of small Tim-like proteins lacking one of the two characteristic disulphide bonds (Figure S1). In summary, the composition of non-opisthokont MPI machineries differs significantly from the classical MPI machineries from yeast and man.

Establishment of *L. tarentolae* as an MPI model system

We then chose the kinetoplastid parasite *L. tarentolae* as an experimental MPI model system for the following reasons:

(i) The parasite is closely related to important pathogens that

cause, for example, African Sleeping Sickness, Chagas disease and different forms of leishmaniasis such as Kala-azar. (ii) *L. tarentolae* liquid cultures are cost-effective and yield sufficient amounts of pure mitochondria for protein import experiments (Brady et al., 1974; Simpson et al., 1996).

To perform a systematic analysis of the MPI in *L. tarentolae*, we cloned *LITOB55*, *LTERTV*, *LTTIM17* and *LTHSP60* as markers for each of the four mitochondrial compartments (Table S1). In addition, a gene encoding a small Tim protein that shares the highest sequence similarity with Tim10 was cloned and named *LtsTIM1* (Table S1 and Figure S1). To confirm the predicted mitochondrial localisations of these components, we purified antibodies against peptides from *LtTob55*, *LtErv*, *LtTim17* and *LtsTim1* (Table S2 and

Table 1 Candidate proteins of the MPI machineries of selected parasitic protists.

Protein	<i>P. falciparum</i> ^a	<i>L. major</i> ^b	<i>T. cruzi</i> ^b
Tob55	PF0410w ^c ?	Q4FXM0	Q4CQ17, Q4CQX2
Tom40	PF0825c	Q4FYU6 ^d ?	Q4DKQ4 ^d ?
Tom22	PFE1230c ^e	-	-
Tom70 ^f	?	?	?
Tim17	PF14_0328	Q4QHR2	Q4DWJ1, Q4E545
Tim23	PF13_0300	?	?
Tim50	PF07_0110	Q4Q9N6 ^g ?	Q4DGU0 ^g ?
Tim22	PF1330c	?	?
Tim9/10 ^h	PF13_0358/PFL0430w	Q4QBW9, Q4Q9T6	Q4E1C1, Q4DQZ7
Tim8/13 ^h	PF14_0208/PFL2065c	Q4QID6, Q4QAR1	Q4D9I4, Q4DJ63
Erv1	PFA0500w	Q4QF88	Q4CWP6
Oxa1	MAL8P1.14	Q4QGW4	Q4E0N8

^aAnnotations are according to PlasmoDB (<http://plasmodb.org/plasmo/>). ^bAnnotations are according to UniProtKB (<http://www.uniprot.org/uniprot/>). Controversial protein properties are labelled with a question mark. ^cThe N-terminal part of the protein might be predicted incorrectly. The protein might start with MNTL. ^dCandidate Q4FYU6 is homologous to Q4DKQ4 from *T. cruzi* (Figure S2) but shares a much lower similarity with yeast Tom40. The primary sequence of the candidates is rather poorly conserved between *Leishmania* and *Trypanosoma* spp. The potential C-terminal targeting sequence seems to be missing in all kinetoplastid but not in the apicomplexan candidates (e.g., residues KFGFMMHI in PFF0825c). ^eThe negatively charged cytosolic receptor domain (recognising positive precursors) is absent. ^fTom70 candidates are difficult to exclude due to the conservation of the tetratricopeptide repeat domain, which is found in numerous proteins (e.g., in ubiquitous Hsp90). ^gThe Tim50 candidates from kinetoplastids are highly altered but have matching peptide patterns (Table 2). In addition, a mitochondrial localisation was predicted for the *T. cruzi* protein using different programs (<http://www.expasy.org/tools/>). Nevertheless, homologies of the candidates to other NIF domain-containing proteins cannot be excluded. ^hSee also Figure S1, Supplementary Results and Discussion 1.

Table 2 Conserved peptide motifs identified by multiple sequence alignments.

Protein	No.	Peptide sequence ^a	Predicted position
Tob55	1	Hy R G F	
	2	(H/F/Q) Hy (F/Y) x ₃ G Po Hy	
	3	G Hy (G/A/V) Hy	
	4	Po Hy E Hy x Hy x ₂ P	
	5 ^b	Hy Po Hy G (L/A/I/V/F) x Hy	
Tim17	1	(D/E) (x ₃ /x ₂) (D/E) P	N-terminal arm ^c
	2	(G/A) x ₂ (F/Y) x ₃ G x ₂ F	Transmembrane segment 2 ^c
	3	R (x/x ₂) (R/K) Po D x (W/Hy) N	Loop/Transmembrane segment 3 ^c
	4	G x ₃ G (G/A) x ₄ R	Transmembrane segment 3 ^c
Tim23	1	R x ₃ (D/E) x (L/A) x (F/Y) x ₂ G	Loop/Transmembrane segment 1 ^d
	2	K x ₃ Hy L N x ₅ G x ₂ Hy (A/G) N	Loop/Transmembrane segment 2 ^d
	3	(D/E) x ₃ Po x ₂ A G x ₃ G x Hy (F/Y) (K/R)	Transmembrane segment 3 ^d
Tim50	1	L L P (D/E/P/L)	
	2	(E/D) (Y/W) x ₄ G (W/Y) (R/K) x ₂ K R P	
	3	(F/Y) E Hy Hy Hy (W/Y/F) Po	
	4	(R/K) D Hy x ₂ L x R	
Tim22	1	G x ₂ Hy G x ₂ Hy G Hy Hy	Transmembrane segment 1
	2	R (x ₂ /x ₃) Po D x ₂ Po x ₃ (A/S) x ₄ G x ₇ G	Loop/Transmembrane segment 3
	3	(S/G/A) F (A/G) Hy F x ₂ Hy Hy (D/E)	Transmembrane segment 4
Tim8, 9, 10, 12, 13	1	C (x/F) x (K/D/x) C	Inner helix (α1)
	2	(E/x) x ₂ C (Hy/x) (D/x) (R/x) C x ₂ (K/R/x)	Outer helix (α2)
Erv1	1	G x ₃ W x ₂ Hy H x ₅ (F/Y)	Helix α1
	2	Y (A/P) C x ₂ C	Active site
	3	H N x Hy N	Helix α4
Oxa1	1	W x ₃ Hy x ₆ Hy R	Transmembrane segment 1 ^e
	2	W Hy x Po L Po x ₂ D (P/x) x ₃ L	Loop/Transmembrane segment 3 ^e

^aHy, hydrophobic amino acid; Po, polar amino acid; x, any amino acid. ^bPlease compare with the motif Po x G x x Hy x Hy by Kutik et al. (2008). The last hydrophobic residue is not conserved in parasites, for example, in the kinetoplastid Tob55 candidates (Table 1) and in kinetoplastid VDAC candidates (data not shown). ^cThe predicted positions are based on alignments using data from Meier et al. (2005). ^dThe predicted positions are based on alignments using data from Rassow et al. (1999). ^eThe predicted positions are based on alignments using data from Herrmann et al. (1997).

Figure S3). All four MPI candidates, as well as the conserved matrix protein *LtHsp60*, were highly enriched in mitochondrial preparations from *L. tarentolae* (Figure 2B,C). Using carbonate extractions, we then confirmed that *LtTob55* and *LtTim17* are integral membrane proteins and that *LtHsp60* is a soluble protein as predicted (Figure 2D). *LtErv* and *LtsTim1* were partially extractable by carbonate, suggesting that both proteins are tightly membrane associated. The expected sub-mitochondrial localisation of *LtTob55*, *LtsTim1*, *LtTim17* and *LtHsp60* was demonstrated by proteolytic susceptibility assays (Figure 2E): The majority of *LtTob55* was cleaved upon addition of proteinase K (PK). Under these conditions, *LtsTim1* and *LtTim17* were protected. When mitochondria were swollen in a hypotonic buffer (Sw), the OM was ruptured and both proteins became susceptible to PK. The matrix protein *LtHsp60* was only degraded when the IM was lysed by the detergent Triton X-100 (TX-100). In order to exclude a localisation of *LtErv* in the endoplasmic reticulum (in analogy to *Erv2* from yeast), we furthermore performed immunogold electron microscopical studies. *LtErv* was detected in the IMS and cristae but not in the endoplasmic reticulum (Figure 2F). In summary, to our knowledge, we established for the first time a kinetoplastid model system with molecular markers for each of the four mitochondrial compartments.

All central MPI pathways are functionally conserved among eukaryotes

We then asked whether radiolabelled versions of our marker proteins *LtHsp60*, *LtTim17*, *LtErv*, *LtsTim1* and *LtTob55* (Figure 2) are correctly imported into isolated mitochondria from *L. tarentolae* or yeast. A time-dependent MPI was detected for all marker proteins and mitochondrial compartments (Figure 3A–E). Moreover, we observed comparable import efficiencies and membrane potential ($\Delta\Psi$) dependencies for mitochondria from both organisms. The results are schematically summarised in Figure 3F. We conclude that the *L. tarentolae* marker proteins are accepted as substrates of the parasite and yeast MPI machineries.

Next, we analysed whether radiolabelled opisthokont model proteins are imported into purified mitochondria from *L. tarentolae*. Yeast mitochondria served as positive controls. Again, a time-dependent MPI was detected for all marker proteins and mitochondrial compartments (Figure 4A–E). The results have important implications, in particular regarding the apparent absence of several opisthokont components hitherto considered indispensable for MPI (Figure 4F). In the following paragraphs, we will therefore compare our results with current MPI models (Neupert and Herrmann, 2007; Chacinska et al., 2009; Endo and Yamano, 2009), starting from the matrix and proceeding stepwise from the IM to the IMS and to the OM.

MPI across the IM into the matrix

The opisthokont matrix marker Su9(1-69)DHFR was not only successfully imported but also processed in *L. tarentolae* mitochondria as demonstrated in Figure 4A. Our data

are in agreement with previous studies on N-terminal matrix targeting signals directing fusion proteins to mitochondria in kinetoplastid (Hauser et al., 1996; Häusler et al., 1997) and apicomplexan parasites (Sato et al., 2003; McMillan et al., 2005; van Dooren et al., 2005). In opisthokonts, proteins with an N-terminal matrix targeting signal are imported by the TIM23 complex, which contains Tim23 and Tim17 as central components. Surprisingly, we and others could not identify Tim23 as well as several additional components of the TIM23 complex *in silico* (Schneider et al., 2008; Singha et al., 2008) (Table 1). Thus, the import and processing machinery for matrix-targeted proteins appear to be functionally conserved despite significant compositional differences. Owing to the absence of Tim23 in kinetoplastid parasites, we suggest that Tim17 was the most important component of the TIM23 complex in the course of evolution. This assumption is supported by mechanistic considerations suggesting that the fundamental mechanism for MPI across the IM might be conserved among eukaryotes, as outlined in the Supplementary Results and Discussion 2.

MPI into the IM

Three different import pathways for IM proteins in opisthokonts have been described (Figure 1B): the OXA, TIM22 and TIM23 pathways. (i) A few IM proteins are inserted from the matrix side via the OXA pathway. This pathway is evolutionary highly conserved (Dolezal et al., 2006; Schneider et al., 2008; Gross and Bhattacharya, 2009; Hewitt et al., 2011), and the central component Oxa1 is also found in parasitic protists (Table 1). (ii) In opisthokonts, Tim22 is the central component of the TIM22 complex, which catalyses the import of IM proteins with multiple transmembrane segments (Figure 1B). In kinetoplastid parasites, we and others could not identify Tim22 *in silico* (Table 1) (Schneider et al., 2008). Nevertheless, the pathway is functionally conserved in the course of evolution as demonstrated in Figures 3B and 4B. This theory is in agreement with a previous study on the import of an AAC homologue from *Entamoeba histolytica* – a member of the amoebozoa (Figure 1A) (Adl et al., 2005) – into yeast mitochondria (Dolezal et al., 2010). (iii) Proteins with a transmembrane segment adjoined to an N-terminal matrix targeting signal are laterally sorted into the IM by the TIM23 complex (Figure 1B). Did1(1-72)DHFR, an artificial marker protein for this so-called stop transfer pathway in opisthokonts, is also imported into *L. tarentolae* mitochondria (Figure 4C). We therefore suggest that the stop transfer pathway also exists in non-opisthokonts. However, owing to the low import efficiencies, we cannot conclude whether such precursors are processed or not. Noteworthy, Tim17/23/22 are homologues (Schneider et al., 2008; Gross and Bhattacharya, 2009; Hewitt et al., 2011) and are also found in other major groups of eukaryotes (e.g., in apicomplexan parasites; Table 1). The identification of only Tim17 in kinetoplastids suggests that the TIM22 complex is absent and that the TIM23 complex is significantly altered in these parasites (Table 1) (Schneider et al., 2008; Singha et al., 2008). In summary, MPI into the IM is functionally conserved despite the apparent absence

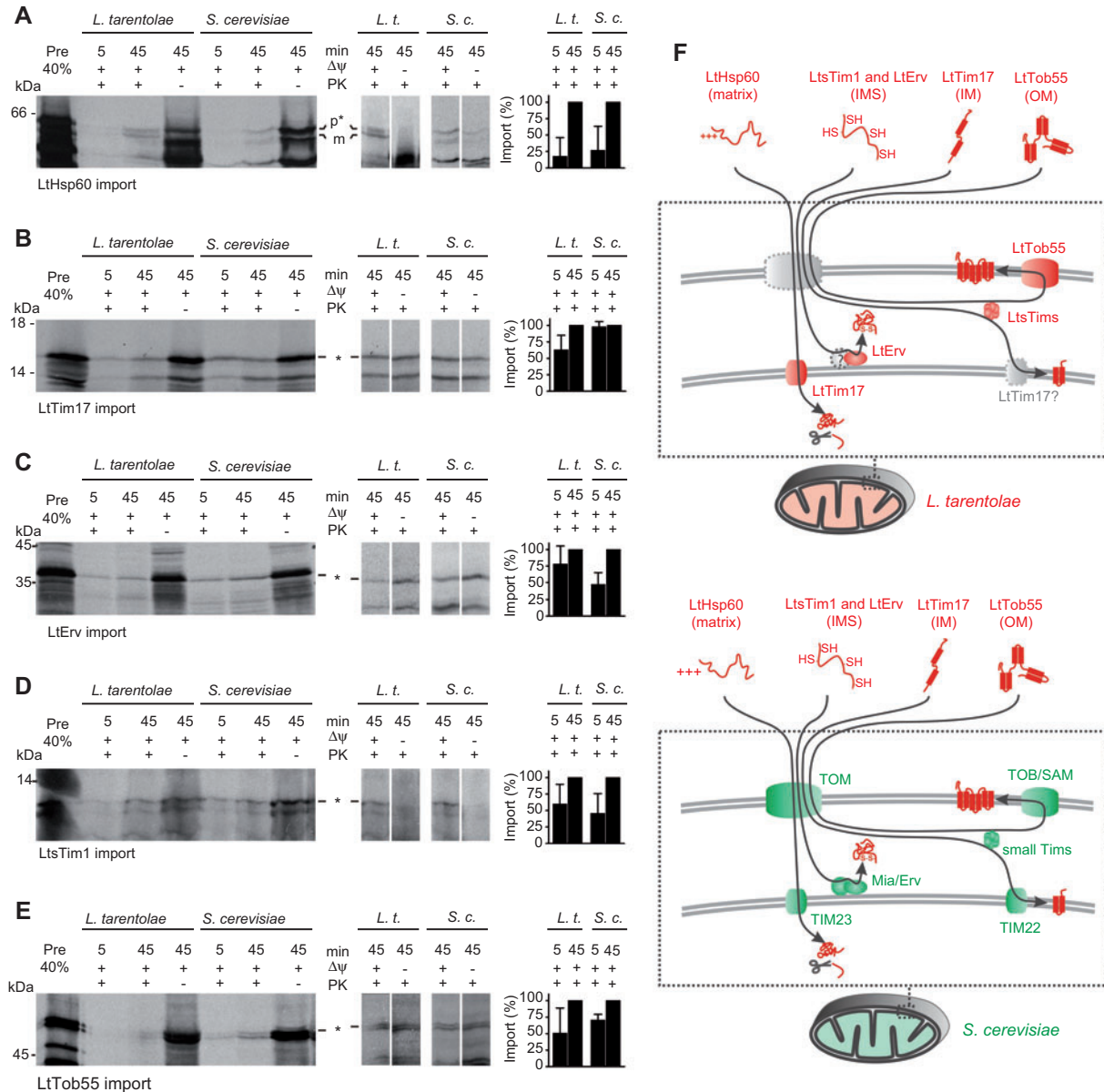


Figure 3 Time- and $\Delta\Psi$ -dependent MPI of *L. tarentolae* marker proteins into parasite and yeast mitochondria.

(A) MPI of the matrix marker protein *LtHsp60* (59.4 kDa). Processing of the precursor (p) upon import into *L. tarentolae* mitochondria yields the mature protein (m) (see also double band in Figure 2C). (B) MPI of the IM marker protein *LtTim17* (16.3 kDa). (C,D) MPI of the IMS marker proteins *LtErv* (34.7 kDa) and *LtsTim1* (11.6 kDa). Import of *LtsTim1* was $\Delta\Psi$ dependent in contrast to the import of *LtErv*. (E) MPI of the OM marker protein *LtTob55* (52.6 kDa). PK treatment was used to remove attached or partially imported proteins. Precursor lysates (Pre) served as controls in all assays. Please note that a few incomplete translation products and/or (proteolytically) truncated proteins were also imported, for example, due to internal or C-terminal import signals. Bands at the expected size of the full-length protein are labelled with an asterisk. The amounts of imported proteins were analysed by autoradiography and densitometric quantification using ImageJ. (F) Schematic summary. MPI of the indicated *L. tarentolae* marker proteins into *L. tarentolae* mitochondria was confirmed experimentally. In addition, all *L. tarentolae* marker proteins were also successfully imported into purified yeast mitochondria.

of Tim23 and TIM22 in kinetoplast parasites (Figures 3F and 4F).

How did the TIM23 and TIM22 machineries evolve? So far, there is no experimental (wet lab) data on the import mechanism of matrix and IM proteins in excavata. Thus, different evolutionary scenarios are plausible (Figure 5A): primitive eukaryotes either already contained (i) the ancestor(s) of

the TIM23 and TIM22 complexes (eukaryote A), (ii) TimX as a precursor of Tim17/23/22 carrying out MPI into the IM and into the matrix (eukaryote B) (Schneider et al., 2008), or (iii) TimX and an unknown component TimZ (eukaryote C). Starting from eukaryote A, the sequence of Tim22 and/or of the TIM receptors could have changed significantly throughout evolution, resulting, for example, in proteins

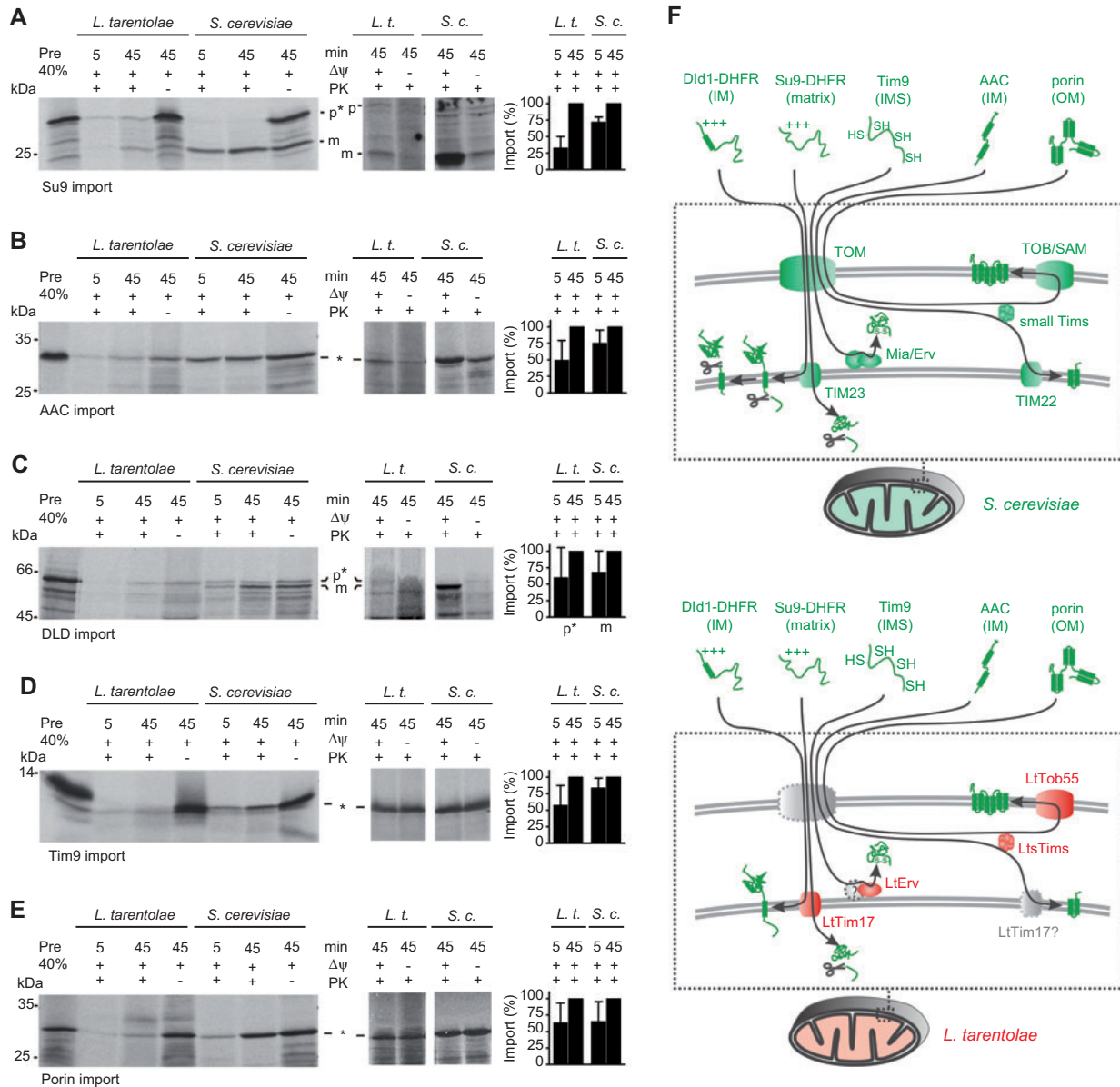


Figure 4 Time- and $\Delta\Psi$ -dependent MPI of opisthokont marker proteins into parasite and yeast mitochondria.

(A) MPI of the artificial matrix marker Su9(1-69)DHFR. The precursor (p) was processed upon $\Delta\Psi$ -dependent import yielding the mature protein (m) in *L. tarentolae* and yeast mitochondria. (B) MPI of the IM marker AAC. In our hands, import of AAC was partially $\Delta\Psi$ dependent for both types of mitochondria. (C) MPI of the artificial IM marker Dld1(1-72)DHFR. Processing of the precursor was not observed in *L. tarentolae* mitochondria despite successful $\Delta\Psi$ -dependent import. (D) MPI of the IMS marker protein Tim9. (E) MPI of the OM marker protein porin. See legend of Figure 3 for details. (F) Schematic summary. MPI of the indicated opisthokont marker proteins into yeast mitochondria served as positive control. In addition, all opisthokont marker proteins were also successfully imported into purified *L. tarentolae* mitochondria although certain import machineries are apparently absent.

Tim22* and Tim50*, which are difficult to identify *in silico* in some eukaryotes (course 1a) in contrast to others (course 1b). Alternatively, Tim22 might have been secondarily lost in some eukaryote lineages (course 2). Starting from eukaryote B, the TIM23 and TIM22 complexes could have evolved from gene duplication events that occurred in several (course 3a) but not all eukaryotes (course 3b). In parallel, the addition of Tim50 and of other putative receptors TimY could reflect similar solutions to the same problem (courses 3a and b, respectively). Alternatively, eukaryotes such as the kinetoplastid parasites

could simply resemble eukaryote B (course 4). Starting from eukaryote C, component TimZ could have been replaced in some eukaryote lineages by Tim22 owing to a TimX gene duplication event (course 5a), whereas in other eukaryotes, such as excavata, TimX was maintained (course 5b).

MPI into the IMS

Owing to the absence of essential Mia40 in parasitic protists (Allen et al., 2008; Deponte and Hell, 2009), it remains

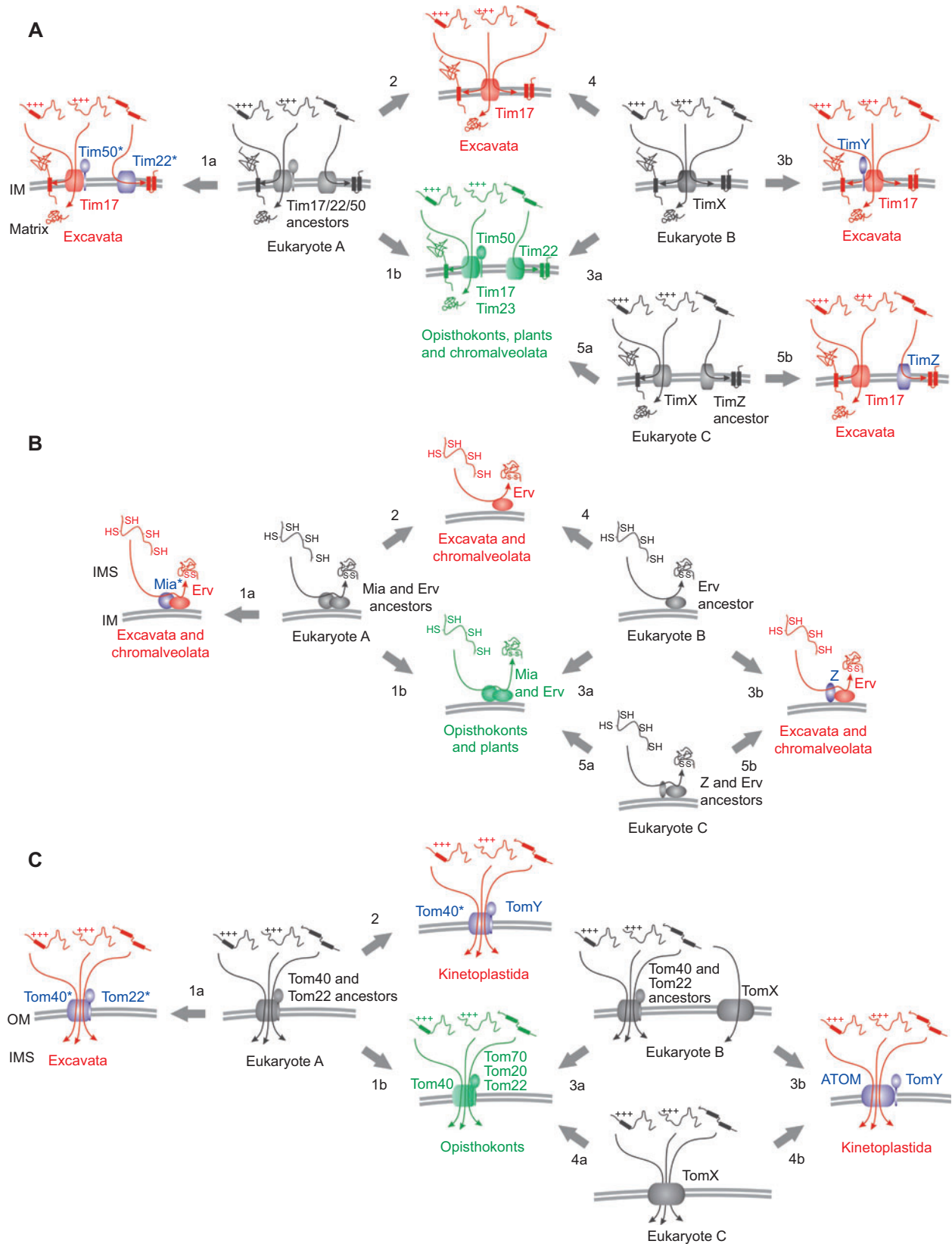


Figure 5 Models on the evolution of MPI machineries.

(A) Evolution of the TIM23 and TIM22 complexes. (B) Evolution of the Mia/Erv system. (C) Evolution of the TOM complex. Putative proteins are highlighted in blue. Hypothetical common ancestors are depicted in grey. The different evolutionary scenarios starting from alternative eukaryotic ancestors A, B, or C are described in the text.

enigmatic how cysteine IMS proteins such as *LtErv* (Figure 3C) and the small *Tims* (Figures 3D and 4D) are imported into parasite mitochondria. Noteworthy, the import of *LtsTim1* was $\Delta\Psi$ dependent in contrast to *LtErv* and *Tim9*. The exact cause of these differences remains to be addressed in future studies. To date, there is no experimental mechanistic data on the MPI of cysteine-containing proteins into the IMS of eukaryotes lacking *Mia40*. Thus, there are three possibilities to explain the functional conservation of the import pathway in the course of evolution (Figure 5B): primitive eukaryotes either contained the ancestor(s) (i) of *Erv* and *Mia40* (eukaryote A), (ii) of *Erv* alone (eukaryote B), or (iii) of *Erv* and an unknown component Z (eukaryote C). Starting from eukaryote A, the sequence of *Mia40* could have changed significantly in the course of evolution, resulting in protein *Mia**, which is difficult to identify *in silico* in some eukaryote lineages (course 1a) in contrast to others (course 1b). Alternatively, *Mia40* became dispensable in some eukaryotes (course 2). Starting from eukaryote B, the acquisitions of *Mia40* and of an unknown component Z could reflect two similar solutions to the same problem (courses 3a and b, respectively). For example, the small *Tim*-like proteins (Figure S1) might be such a component Z. Of course, current eukaryotes without *Mia40* could also resemble eukaryote B (course 4). For example, *LtErv* – which has an alternative cysteine pattern and an additional C-terminal domain (Deponete and Hell, 2009) – might not require another partner (Allen et al., 2008; Deponete and Hell, 2009). Alternatively, starting from eukaryote C, component Z could have been replaced by *Mia40* in several (course 5a) but not all eukaryotes (course 5b). In summary, we are just at the beginning of deciphering MPI into the IMS of parasitic protists (Figures 3F and 4F).

MPI across and into the OM

We showed that a set of different opisthokont and kinetoplastid proteins is successfully transported across the OM of *L. tarentolae* mitochondria (Figures 3 and 4). Thus, there is either an unspecific pore in the OM or a kind of TOM complex that recognises mitochondrial proteins from different species. The latter possibility is supported by the fact that the TOM complex of yeast also seems to lack species specificity regarding MPI of kinetoplastid proteins (Figure 3). However, it was previously suggested that the β -barrel protein *Tom40* has been lost in kinetoplastids (Schneider et al., 2008; Pusnik et al., 2009), and we could not identify a *bona fide* *Tom40* candidate in these organisms either (apart from a putative homologue from *Trypanosoma cruzi* shown in Figure S2). In line with these findings, an alternative translocase of the *Omp85* superfamily, named *ATOM*, was reported during the preparation of our manuscript by Pusnik et al. (2011). Our opisthokont and kinetoplastid proteins therefore probably entered the *L. tarentolae* mitochondria with the help of *ATOM*. With respect to the integration of β -barrel proteins, *LtTob55* and porin were both successfully imported into the OM of opisthokont and *L. tarentolae* mitochondria (Figures 3E and 4E). Thus, there is a functionally conserved TOB/SAM complex in kinetoplastids.

Our results support the theory that the MPI of β -barrel proteins is highly conserved throughout evolution (Gross and Bhattacharya, 2009; Walther et al., 2009; Hewitt et al., 2011). Another remarkable aspect is the apparent absence of genes encoding classical TOM and TOB/SAM receptors (Table 1), as these are required for the recognition of mitochondrial targeting signals in opisthokonts (Neupert and Herrmann, 2007; Chacinska et al., 2009; Endo and Yamano, 2009). One explanation could be that the average matrix targeting signals of parasitic protists – although functionally conserved (Figure 3A) – differ significantly from opisthokont signals with respect to their length and/or amino acid composition (Hauser et al., 1996; Schneider et al., 2008). The parasite import receptors might therefore be different as well. Indeed, previous *in silico* analyses suggested that the receptors *Tom20* and *Tom70* are restricted to opisthokonts (Hewitt et al., 2011). Furthermore, the highly negatively charged cytosolic receptor domain of *Tom22* also seems to be absent in non-opisthokonts (e.g., in *Plasmodium*; Table 1). In summary, general MPIs across the OM and the MPI of β -barrel proteins into the OM are both functionally conserved. However, so far, we know very little about the composition of the (A)TOM complex in kinetoplastids and about the recognition of mitochondrial proteins at the parasite OM. If there are specialised cytosolic or IMS receptor domains, they presumably have similar properties to the opisthokont receptors despite alternative primary structures.

How did the TOM complex evolve? So far, no parasite TOM complex has been biochemically characterised with respect to both its composition and function. However, based on the considerations stated above, primitive eukaryotes either contained the ancestors (i) of classical TOM core components alone (eukaryote A), (ii) of TOM core components and a component *TomX* (eukaryote B), or (iii) of an ancestral pore formed by *TomX* (eukaryote C) (Figure 5C). Starting from eukaryote A, the sequence of *Tom40* and of *Tom* receptors could have changed significantly in the course of evolution resulting in, for example, *Tom40**, which is difficult to identify *in silico* in some eukaryote lineages (course 1a) in contrast to others (course 1b). For example, β -barrel candidates from *E. histolytica* (as a member of the amoebozoa) or from the excavate *Giardia* have very low overall sequence similarities with *Tom40* from opisthokonts (Dagley et al., 2009; Dolezal et al., 2010). In addition, some TOM receptors could have been replaced by so far unknown components (course 2). Starting from eukaryote B, the ancestor of *Tom40* in opisthokonts (course 3a) could have been replaced in some eukaryotes due to a functional overlap with component *TomX* (course 3b). Starting from eukaryote C, *Tom40* could have been acquired secondarily in many (course 4a) but not all eukaryotes (course 4b). Based on very recent findings, *TomX* is an ancestor of *ATOM* in kinetoplastids, suggesting a bacterial origin of this component (Pusnik et al., 2011). Although courses 3b and 4b are both possible, Pusnik et al. favoured eukaryote C as the last common ancestor with respect to the evolution of *ATOM* and *Tom40*. The scenarios depicted in Figure 5 obviously need to be tested experimentally.

Conclusions

Regarding all the differences summarised above, we suggest that alternative or even novel MPI components and mechanisms are likely to be identified in parasitic protists. Owing to the lack of experimental data on non-opisthokont MPI machineries, we cannot discriminate between different evolutionary scenarios yet. Previous and future *in silico* analyses certainly provide an excellent starting point for deciphering MPI in non-opisthokonts. However, they predominantly lead to the identification of homologues or peptide patterns of already known components. Much more experimental work is necessary to confirm or exclude the existence of novel MPI components and altered MPI pathways in parasitic protists. On the one hand, results from such studies might reveal valuable targets to combat these pathogens. On the other hand, studies on kinetoplastid parasites have also often led to significant advances in cell biology, regarding, for example, glycosylphosphatidylinositol anchors (Ferguson, 1999) as well as RNA editing and splicing (Knoop, 2011). The analyses of parasite protein transport machineries might therefore also be helpful to learn more about the mechanisms of MPI in opisthokonts.

Materials and methods

BLAST searches, sequence alignments and peptide pattern identification

The databases EuPathDB, PlasmoDB and GeneDB (<http://eupathdb.org/eupathdb/>; <http://plasmodb.org/plasmo/>; <http://www.genedb.org/>) were searched for open reading frames encoding putative MPI machinery components from kinetoplastid (*T. brucei*, *T. cruzi*, *L. major*, *L. braziliensis* and *L. infantum*) and apicomplexan parasites (*Plasmodium* spp. and *T. gondii*). Yeast and *N. crassa* MPI components were used as input sequences for BLAST and hidden Markov model searches. Identified parasite candidate genes were translated and used for (i) cross-BLAST searches in closely related organisms, (ii) reciprocal BLAST analyses against opisthokont genome database and (iii) general TBLASTN searches against eukaryote genomes (<http://blast.ncbi.nlm.nih.gov/Blast.cgi>; <http://www.ebi.ac.uk/Tools/sss/>). For some genes, direct BLAST analyses gave a significant hit with only one organism. Homologues in related organisms were subsequently identified by cross-BLAST analyses. Candidates that could not be confirmed in reciprocal BLAST analyses were discarded. To identify conserved peptide motifs for additional database searches, selected candidates from TBLASTN searches were used as input sequences for multiple sequence alignments with homologues from non-related eukaryotes (<http://www.ebi.ac.uk/Tools/msa/>). Identified peptide patterns were generalised and confirmed in additional search cycles against eukaryote genomes. Best results were obtained when BLAST, hidden Markov model and peptide motif searches were combined.

Cloning of candidate genes

Full-length *LITOB55*, *LTERTV*, *LTTIM17*, *LTsTIM1* and *LTHSP60* were PCR amplified from genomic *L. tarentolae* DNA with *Pfu* polymerase (Promega, Mannheim, Germany) and cloned into the vector pDrive using the PCR cloning and A-addition kits from Qiagen (Hilden, Germany). Primers (Metabion International, Martinsried, Germany) are listed in Table S1. The gene sequences have been

deposited in GenBank (<http://www.ncbi.nlm.nih.gov/genbank/>) under accession numbers JN380346–JN380350. For *in vitro* transcription/translation experiments, all genes were subcloned into pGEM4 using *EcoRI* restriction sites. Orientation and sequences of all inserts and plasmids were checked by restriction analysis and by sequencing both strands.

Generation and purification of antibodies

Rabbits were immunised with the synthetic peptides given in Table S2 (Pineda Antibody Service, Berlin, Germany). Antibodies were purified from sera by affinity chromatography using borohydride-reduced peptide (in 50 mM Tris/HCl, 5 mM EDTA, pH 8.5) that was coupled for 45 min to 1 ml SulfoLink resin (Pierce, Bonn, Germany). Chromatography and elution were performed according to the manufacturer's instructions. Antibody-containing eluate fractions were identified by Western blotting against *L. tarentolae* cell lysates and purified mitochondria (Figure S3).

Purification of mitochondria from *L. tarentolae*

Yeast mitochondria were purified as described previously (Harner et al., 2011). *L. tarentolae* mitochondria were purified from mid-log phase liquid cultures by differential centrifugation and density gradient ultracentrifugation: 3–6 l of parasite cultures ($5\text{--}9 \times 10^7$ cells/ml) were centrifuged for 10 min in 1 l buckets at $4000 \times g$, 4°C , and washed with 250 ml ice-cold buffer (10 mM Tris/HCl, 0.15 M NaCl, 0.1 mM EDTA, pH 7.9) per litre of culture. All following steps were performed with ice-cold solutions. Cells were ruptured in hypotonic swelling buffer (1 mM Tris, pH 7.9, 1 mM EDTA, containing complete EDTA-free protease inhibitor cocktail from Roche, Mannheim, Germany) by passing through a 0.4 mm \varnothing needle at 6 bar. The lysate was immediately supplemented with 7.5% sucrose and centrifuged for 10 min at $16\,000 \times g$, 4°C . The pellet was resuspended in 20 mM Tris, pH 7.9, 0.25 M saccharose and 2 mM MgCl_2 . MgCl_2 (1 M) was added to a final concentration of 3 mM, and the suspension was treated for 30 min with 30 U/ml DNase I. Two volumes of STE buffer (0.25 M saccharose, 20 mM Tris, 2 mM EDTA, pH 7.9) were added and the suspension was centrifuged for 10 min at $16\,000 \times g$, 4°C . The pellet was dissolved in 4 ml 50% Histodenz, 0.25 M saccharose, 20 mM Tris, 0.1 mM EDTA, pH 7.9 per litre of culture, loaded under a Histodenz gradient (31.6%, 28.3%, 25% and 21.7%), and fractions were separated by ultracentrifugation for 2 h at $104\,000 \times g$, 4°C . The mitochondrial fraction was harvested, diluted in 5 volumes of STE buffer and centrifuged for 10 min at $32\,500 \times g$, 4°C . Mitochondria were resuspended in STE buffer to a final concentration of 5–10 mg/ml. The protein content and the suborganellar localisation were analysed by proteolytic susceptibility assays, SDS-PAGE and Western blotting (Harner et al., 2011) using our affinity-purified rabbit peptide antibodies (Figure S3).

Carbonate extraction

Carbonate extractions were performed with fraction 4 of purified mitochondria (Figure 2B). Two samples of mitochondria (50–100 μg) were centrifuged for 10 min at $12\,000 \times g$, 4°C . One pellet was directly resuspended in 20 μl Laemmli buffer (total). The second pellet was resuspended in 50 μl of 20 mM Tris, pH 7.2 and supplemented with 50 μl 200 mM Na_2CO_3 . The suspension was vortexed for 15 s, incubated for 30 min on ice and centrifuged for 30 min at $155\,000 \times g$, 4°C . The pellet was directly resuspended in 20 μl Laemmli buffer (pellet). The supernatant was precipitated with 20 μl 72% trichloroacetic acid (TCA) for 30 min at -80°C , washed with acetone and

resuspended in 20 μ l Laemmli buffer (supernatant). Proteins were detected by SDS-PAGE and Western blotting (Harner et al., 2011) using our affinity-purified rabbit peptide antibodies (Figure S3).

Electron microscopy

Cells were prepared for immuno-electron microscopy using the 'Tokuyasu' method (Griffiths, 1993). Briefly, mid-log phase promastigotes were fixed at room temperature for 1 h with 4% paraformaldehyde, 0.1% glutaraldehyde in 60 mM Pipes, 25 mM Hepes, 2 mM $MgCl_2$, 10 mM EGTA, pH 6.9 and incubated for 10 min with 50 mM glycine in PBS. The parasites were centrifuged for 5 min at 2000 \times g and washed and resuspended in 10% gelatin in PBS that was subsequently hardened on ice. Small gelatin blocks were incubated with 2.3 M sucrose overnight, and then frozen in liquid nitrogen. Thin cryosections (100 nm) were cut using a Leica EM UC6 Ultramicrotome, and sections were fixed on carbon-coated copper grids. For immunolabelling, sections were blocked for 30 min on blocking solution (0.8% BSA, 0.1% fish skin gelatin, 1% glutaraldehyde, 50 mM glycine, PBS), incubated for 30 min with *LtErv* peptide antibody (diluted 1:10 in blocking solution) and incubated for 20 min with 10 nm protein A gold (diluted 1:70 in blocking solution). The sections were contrasted with 0.45% uranyl acetate and embedded in 1.7% methyl cellulose in H_2O . The images were recorded using Tecnai F30 (FEI) and Zeiss EM900 microscopes on slow-scan 2k \times 2k CCD cameras.

Radioactive MPI assays

Radiolabelled precursors were synthesised as described previously (Harner et al., 2011) using pGEM4 constructs (under control of the SP6 promoter), [^{35}S]-methionine (MP Biomedicals, Eschwege, Germany) and the TNT Coupled Reticulocyte Lysate System (Promega) according to the manufacturer's instructions. Except for the following modifications, import assays were performed as described previously (Harner et al., 2011). (i) We used *L. tarentolae* mitochondria in STE buffer. (ii) Imports were performed in the presence of 1 mM ATP, 5 mM NADH, 5 mM succinate, 0.08 mg/ml creatine kinase and 6 mM creatine phosphate. (iii) Imports were stopped on ice by adding 400 μ l 10 mM MOPS, 250 mM saccharose, 80 mM KCl, 1 mM EDTA, pH 7.2 and 5 μ l PK (10 mg/ml). (iv) Mitochondria were re-isolated by centrifugation for 15 min at 21 000 \times g, 4°C. Import efficiencies decreased significantly when frozen parasite mitochondria were used. Accordingly, all assays were performed with fresh preparations of fraction 4 (Figure 2B,C). Imported proteins were visualised by SDS-PAGE, blotting and autoradiography using Kodak BioMax MR films (Sigma, Taufkirchen, Germany). All import experiments were repeated at least three times.

Supplementary data

Supplementary Tables S1 and S2, Figures S1–S3 and Results and Discussion are available online at <http://dx.doi.org/10.1515/hzs-2011-0255SUP>. Novel sequence data have been deposited in GenBank (<http://www.ncbi.nlm.nih.gov/genbank/>) under accession numbers JN380346–JN380350.

Acknowledgments

We thank S. Mittler for help with sequence analyses, W. Neupert and A. Simpson for initial support, A. Schneider for starting cultures,

K. Hell for materials and discussions and J. Riemer for critically reading the manuscript. This work was primarily supported by the Deutsche Forschungsgemeinschaft (grant DE 1431/2 to M.D.). Additional support came from the Bavaria California Technology Center and the Friedrich-Baur-Foundation (to M.D.).

References

- Adl, S.M., Simpson, A.G., Farmer, M.A., Andersen, R.A., Anderson, O.R., Barta, J.R., Bowser, S.S., Brugerolle, G., Fensome, R.A., Fredericq, S., et al. (2005). The new higher level classification of eukaryotes with emphasis on the taxonomy of protists. *J. Eukaryot. Microbiol.* 52, 399–451.
- Allen, J.W., Ferguson, S.J., and Ginger, M.L. (2008). Distinctive biochemistry in the trypanosome mitochondrial intermembrane space suggests a model for stepwise evolution of the MIA pathway for import of cysteine-rich proteins. *FEBS Lett.* 582, 2817–2825.
- Baker, M.J., Webb, C.T., Stroud, D.A., Palmer, C.S., Frazier, A.E., Guiard, B., Chacinska, A., Gulbis, J.M., and Ryan, M.T. (2009). Structural and functional requirements for activity of the Tim9-Tim10 complex in mitochondrial protein import. *Mol. Biol. Cell* 20, 769–779.
- Braly, P., Simpson, L., and Kretzer, F. (1974). Isolation of kinetoplast-mitochondrial complexes from *Leishmania tarentolae*. *J. Protozool.* 21, 782–790.
- Cavalier-Smith, T. (2010). Kingdoms Protozoa and Chromista and the eozoan root of the eukaryotic tree. *Biol. Lett.* 6, 342–345.
- Chacinska, A., Koehler, C.M., Milenkovic, D., Lithgow, T., and Pfanner, N. (2009). Importing mitochondrial proteins: machineries and mechanisms. *Cell* 138, 628–644.
- Dagley, M.J., Dolezal, P., Likic, V.A., Smid, O., Purcell, A.W., Buchanan, S.K., Tachezy, J., and Lithgow, T. (2009). The protein import channel in the outer mitochondrial membrane of *Giardia intestinalis*. *Mol. Biol. Evol.* 26, 1941–1947.
- Deponte, M. and Hell, K. (2009). Disulphide bond formation in the intermembrane space of mitochondria. *J. Biochem.* 146, 599–608.
- Dolezal, P., Likic, V., Tachezy, J., and Lithgow, T. (2006). Evolution of the molecular machines for protein import into mitochondria. *Science* 313, 314–318.
- Dolezal, P., Dagley, M.J., Kono, M., Wolyneć, P., Likic, V.A., Foo, J.H., Sedinova, M., Tachezy, J., Bachmann, A., Bruchhaus, I., et al. (2010). The essentials of protein import in the degenerate mitochondrion of *Entamoeba histolytica*. *PLoS Pathog.* 6, e1000812.
- Embley, T.M. and Martin, W. (2006). Eukaryotic evolution, changes and challenges. *Nature* 440, 623–630.
- Endo, T. and Yamano, K. (2009). Multiple pathways for mitochondrial protein traffic. *Biol. Chem.* 390, 723–730.
- Ferguson, M.A. (1999). The structure, biosynthesis and functions of glycosylphosphatidylinositol anchors, and the contributions of trypanosome research. *J. Cell Sci.* 112, 2799–2809.
- Gentle, I.E., Perry, A.J., Alcock, F.H., Likic, V.A., Dolezal, P., Ng, E.T., Purcell, A.W., McConville, M., Naderer, T., Chanez, A.L., et al. (2007). Conserved motifs reveal details of ancestry and structure in the small TIM chaperones of the mitochondrial intermembrane space. *Mol. Biol. Evol.* 24, 1149–1160.
- Griffiths, G. (1993). *Fine Structure Immunocytochemistry*. (Heidelberg, Germany: Springer-Verlag).
- Gross, J. and Bhattacharya, D. (2009). Mitochondrial and plastid evolution in eukaryotes: an outsiders' perspective. *Nat. Rev. Genet.* 10, 495–505.

- Harner, M., Neupert, W., and Deponte, M. (2011). Lateral release of proteins from the TOM complex into the outer membrane of mitochondria. *EMBO J.* *30*, 3232–3241.
- Hauser, R., Pypaert, M., Häusler, T., Horn, E.K., and Schneider, A. (1996). *In vitro* import of proteins into mitochondria of *Trypanosoma brucei* and *Leishmania tarentolae*. *J. Cell Sci.* *109*, 517–523.
- Häusler, T., Stierhof, Y.D., Blattner, J., and Clayton, C. (1997). Conservation of mitochondrial targeting sequence function in mitochondrial and hydrogenosomal proteins from the early-branching eukaryotes *Crithidia*, *Trypanosoma* and *Trichomonas*. *Eur. J. Cell Biol.* *73*, 240–251.
- Herrmann, J.M., Neupert, W., and Stuart, R.A. (1997). Insertion into the mitochondrial inner membrane of a polytopic protein, the nuclear-encoded Oxa1p. *EMBO J.* *16*, 2217–2226.
- Hewitt, V., Alcock, F., and Lithgow, T. (2011). Minor modifications and major adaptations: the evolution of molecular machines driving mitochondrial protein import. *Biochim. Biophys. Acta* *1808*, 947–954.
- Knoop, V. (2011). When you can't trust the DNA: RNA editing changes transcript sequences. *Cell. Mol. Life Sci.* *68*, 567–586.
- Kutik, S., Stojanovski, D., Becker, L., Becker, T., Meinecke, M., Krüger, V., Prinz, C., Meisinger, C., Guiard, B., Wagner, R., et al. (2008). Dissecting membrane insertion of mitochondrial β -barrel proteins. *Cell* *132*, 1011–1024.
- Lill, R. (2009). Function and biogenesis of iron-sulphur proteins. *Nature* *460*, 831–838.
- McMillan, P.J., Stimmler, L.M., Foth, B.J., McFadden, G.I., and Müller, S. (2005). The human malaria parasite *Plasmodium falciparum* possesses two distinct dihydrolipoamide dehydrogenases. *Mol. Microbiol.* *55*, 27–38.
- Meier, S., Neupert, W., and Herrmann, J.M. (2005). Conserved N-terminal negative charges in the Tim17 subunit of the TIM23 translocase play a critical role in the import of preproteins into mitochondria. *J. Biol. Chem.* *280*, 7777–7785.
- Neupert, W. and Herrmann, J.M. (2007). Translocation of proteins into mitochondria. *Annu. Rev. Biochem.* *76*, 723–749.
- Pusnik, M., Charrière, F., Mäser, P., Waller, R.F., Dagley, M.J., Lithgow, T., and Schneider, A. (2009). The single mitochondrial porin of *Trypanosoma brucei* is the main metabolite transporter in the outer mitochondrial membrane. *Mol. Biol. Evol.* *26*, 671–680.
- Pusnik, M., Schmidt, O., Perry, A.J., Oeljeklaus, S., Niemann, M., Warscheid, B., Lithgow, T., Meisinger, C., and Schneider, A. (2011). Mitochondrial preprotein translocase of trypanosomatids has a bacterial origin. *Curr. Biol.* *21*, 1738–1743.
- Rassow, J., Dekker, P.J., van Wilpe, S., Meijer, M., and Soll, J. (1999). The preprotein translocase of the mitochondrial inner membrane: function and evolution. *J. Mol. Biol.* *286*, 105–120.
- Sato, S., Rangachari, K., and Wilson, R.J. (2003). Targeting GFP to the malarial mitochondrion. *Mol. Biochem. Parasitol.* *130*, 155–158.
- Schneider, A., Bursac, D., and Lithgow, T. (2008). The direct route: a simplified pathway for protein import into the mitochondrion of trypanosomes. *Trends Cell Biol.* *18*, 12–18.
- Simpson, L., Frech, G.C., and Maslov, D.A. (1996). RNA editing in trypanosomatid mitochondria. *Methods Enzymol.* *264*, 99–121.
- Singha, U.K., Peparah, E., Williams, S., Walker, R., Saha, L., and Chaudhuri, M. (2008). Characterization of the mitochondrial inner membrane protein translocator Tim17 from *Trypanosoma brucei*. *Mol. Biochem. Parasitol.* *159*, 30–43.
- Smid, O., Matusková, A., Harris, S.R., Kucera, T., Novotný, M., Horváthová, L., Hrdý, I., Kutejová, E., Hirt, R.P., Embley, T.M., et al. (2008). Reductive evolution of the mitochondrial processing peptidases of the unicellular parasites *Trichomonas vaginalis* and *Giardia intestinalis*. *PLoS Pathog.* *4*, e1000243.
- Tsaousis, A.D., Gaston, D., Stechmann, A., Walker, P.B., Lithgow, T., and Roger, A.J. (2011). A functional Tom70 in the human parasite *Blastocystis* sp.: implications for the evolution of the mitochondrial import apparatus. *Mol. Biol. Evol.* *28*, 781–791.
- van Dooren, G.G., Marti, M., Tonkin, C.J., Stimmler, L.M., Cowman, A.F., and McFadden, G.I. (2005). Development of the endoplasmic reticulum, mitochondrion and apicoplast during the asexual life cycle of *Plasmodium falciparum*. *Mol. Microbiol.* *57*, 405–419.
- van Dooren, G.G., Stimmler, L.M., and McFadden, G.I. (2006). Metabolic maps and functions of the *Plasmodium* mitochondrion. *FEMS Microbiol. Rev.* *30*, 596–630.
- Walther, D.M., Papic, D., Bos, M.P., Tommassen, J., and Rapaport, D. (2009). Signals in bacterial β -barrel proteins are functional in eukaryotic cells for targeting to and assembly in mitochondria. *Proc. Natl. Acad. Sci. USA* *106*, 2531–2536.

Received November 9, 2011; accepted February 20, 2012

Supplemental data

Supplementary results and discussion 1: identification and classification of novel small Tims

Tim8/Tim13 and Tim9/Tim10 form $\alpha_3\beta_3$ hexamers and guide proteins across the IMS to the TOB and the TIM22 complex (Figure 1B) (Baker et al., 2009; Chacinska et al., 2009; Endo and Yamano, 2009; Neupert and Herrmann, 2007). The small Tims have two characteristic Cx_3C motifs (a so-called twin Cx_3C motif), which are recognised and oxidised by the Mia40/Erp1 couple (Figure S1) (Deponte and Hell, 2009). As reported previously (Gentle et al., 2007), homologues of all four opisthokont small Tims are present in some apicomplexan parasites, whereas others might have lost up to three of the proteins. In kinetoplastids, we found four candidates for small Tims (Table 1), which is one more than in previous studies (Gentle et al., 2007). The sequence similarity of the fourth protein is lower, and the loop connecting the two predicted Cx_3C -containing α -helices is enlarged (Figure S1), which might be the reason why it has been overlooked so far. Kinetoplastids furthermore have a small Tim-like protein lacking the first disulphide bridge (Q4DDD2 and Q4Q3B2 in *Trypanosoma cruzi* and *Leishmania major*, respectively). The alignment of the small Tims in Figure S1 reveals that some of the candidates cannot be unambiguously assigned: for example, the protein Q4QAR1 from *L. major* was previously classified as a homologue of Tim9 (CAJ03937) (Gentle et al., 2007), and the first motif (ExCFNLC x_2 E) indeed resembles Tim9 from yeast. However, the second motif

(KxEx $_2$ CIDRC x_2 RY) is far more similar to Tim10/Tim12, and both motifs are separated by 16 instead of 15 residues. In summary, the unusual repertoire of small Tims and the absence of Mia40 suggest that the IMS import machineries of parasitic protists differ significantly from their vertebrate hosts.

Supplementary results and discussion 2: the molecular mechanism of Tim17

So far, only few data on the Tim17-dependent MPI mechanism is available. Two functionally highly relevant negative charges at the N-terminal arm of yeast Tim17 were suggested to interact with two positive charges of an internal loop in the IMS (Meier et al., 2005). The intramolecular ionic interaction could then be replaced by the interaction with the positive charges of matrix precursor proteins during import. Indeed, the positive charges of residues Arg83 and Arg85 in yeast Tim17 are highly conserved and are also found in homologues from kinetoplastid and apicomplexan parasites (peptide 3 in Table 2). The acidic residues at the N-terminus of Tim17 are also conserved and are in front of a proline residue in a (D/E) x_3 (D/E)P motif in opisthokonts and apicomplexan parasites. In kinetoplastid parasites, the motif is replaced by the sequence (D/E) x_5 (D/E)P (peptide 1 in Table 2). In summary, MPI into the matrix could be functionally as well as mechanistically conserved.


```

Sc  ----MSAPTPLAEEASQIPTIPALSPLTAKQSKGNFFSSNPIS--SFVVDTYKQLHSHRQ  53
Tc  MDVSVVLAADVLSSSDTRHALILVGRQSVAGGSGNQEQAVCIVSDAIPCTDMDVIMEQVE  60
      : * . * : : . . : : . . . . * * . : * : : . : : :
Sc  SLELVNPGTVENLNKEVSRDVFLSQYFFTGLRADLNKAFSMNPAFQTSHTFS--IGSQAL  111
Tc  CLEQVLPCGIAFLGVFLPGDGVKD---LAALRHSLSSHLQVSSFFVAKYDNEGRVQCRL  117
      . * * * * : * . : . * . . : : * * . * . : : . . * : : . : : *
Sc  PKYAFSALFANDNLFAQGNIDN-DLSVSGRLNYGWDKKNISKVNLQISDGQPTMCQLEQD  170
Tc  QSGRMLSVTTPDTKPVLVTLACYFFSPLGQFPFIVRSKDENITSNVLLDVTSTALMEHNQ  177
      . : : : * . . : : : * * : : . * : . . . : * . * : : :
Sc  YQASDFSVNVKTLNPSFSEKGEFTGVAVASF-LQSVTPQLALGLETLYSRTDGSAPGDAG  229
Tc  IWDSVDALYAVQLGSTEGQEMLCVHVTFFPFLSCGQGVYRAICTLLPKVERRRPQVMV  237
      * : : . * . : : : * : * * : * : * : : : * * : : : .
Sc  VSYLTRYVSKKQDWIFSGQLQANGALIASLWRKVAQNVEAGIETTLQAGMVPITDPLMGT  289
Tc  RVGSRRYPSLVYQWIFTPTERGSAALSVKQWDELRELIEDGVGEEVQPSQV-VTDTF  296
      * * * : * * : : * * . . * : : : * * : * . . * : * * : * .
Sc  PIG-IQPTVEGSTTIGAKYEYRQSVYRGTLDNSNGKVACFLERKVLPTLSVLFCGEIDHFK  348
Tc  PSATASTTIEGSTNMRNKTAQASEVSN--TFQREKAKGDFLR--YMPPLLVLFCSLFLYFC  352
      * . . * : * * * : * : : * : : . * * . : * . * * * . : *
Sc  NDTKIGCGLQFETAGNQELMLLQQLDADGNPLQALPQL  387
Tc  CTK----- 355

```

Figure S2 Sequence alignment of Tom40 from *Saccharomyces cerevisiae* and a putative candidate protein from *T. cruzi*. The *T. cruzi* sequence corresponds to hypothetical protein Q4DKQ4 (UniProtKB annotation, <http://www.uniprot.org/uniprot/>). The targeting sequence of yeast Tom40 is shaded black (Kutik et al., 2008). The signal is absent in the parasite candidate.

Table S1 Primers used for cloning of *Leishmania tarentolae* candidate genes.

Construct	Annotation	Primer	Sequence
<i>LITOB55</i> /pDrive	JN380346	Sense	5'-ATGACCGACTATGCAACAAACGGTAAACATTTGTGAGG-3'
		Antisense	5'-CTAGAACGAGAAATTGGATGACCAAACCAAACCAAACCGGAACCGATC-3'
<i>LITERV</i> /pDrive	JN380347	Sense	5'-ATGTCGGACGACGACGTACACGAACGCCTCACCACCATCCC-3'
		Antisense	5'-CTAGAGCTTGAGTCTTCGTCCTCTGGCAGTACACTTG-3'
<i>LTTIM17</i> /pDrive	JN380349	Sense	5'-ATGACATCCATCTTGGACCCTAGGC-3'
		Antisense	5'-TTAGTGCTGGGCCATGCCATGGC-3'
<i>LtTIM1</i> /pDrive	JN380348	Sense	5'-ATGCAGCCGGTGCAGTCAATCCGAGCCTCATGGGGCTGACGC-3'
		Antisense	5'-TCACATTTTACCCGCTGCTGCGTCTTCATCCACTGATACGG-3'
<i>LTHSP60</i> /pDrive	JN380350	Sense	5'-ATGCTCCGCTCCGCTGTGTGCTTGCAG-3'
		Antisense	5'-CTAGAAGCCCATGCCGCCCATGCCGCC-3'

Table S2 Peptide sequences used for rabbit immunisation and antibody purification.

Protein	Annotation	Position	Sequence
<i>LtTob55</i>	JN380346	Residues 182–200 of 473	H ₂ N-CRVEEVKATTTNRKGLASE-CONH ₂
<i>LtErv</i>	JN380347	Residues 115–133 of 312	H ₂ N-CLRRWHPGYPNKMEDTPTIE-CONH ₂
<i>LtTim17</i>	JN380349	Residues 61–78 of 152	H ₂ N-CTADFFRHSLRSAHRLGGS-CONH ₂
<i>LtTim1</i>	JN380348	Residues 40–57 of 102	H ₂ N-CITHYGDDAIPYHPGEKA-CONH ₂

If necessary, an additional cysteine residue (underlined) was added to the N-terminus of the synthetic peptide for peptide coupling before affinity chromatography.

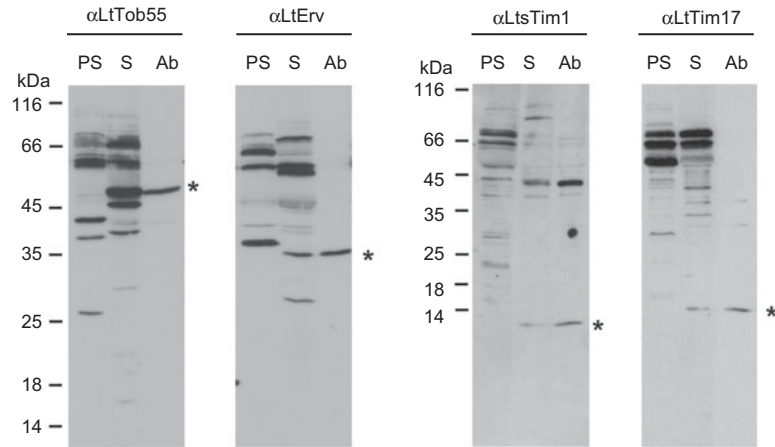


Figure S3 Purification of antibodies against mitochondrial marker proteins from *L. tarentolae*. Antibodies against the proteins *LtTob55*, *LtErv*, *LtsTim1* and *LtTim17* were purified by affinity chromatography using the respective peptides listed in Table S2. The quality of the preparations was monitored by Western blot analyses using preimmune serum (PS), serum (S), and affinity purified antibodies (Ab). In each lane, 50 μ g of mitochondrial proteins from *L. tarentolae* was separated by gel electrophoresis using either 12% SDS-polyacrylamide gels (left panels) or 8 M urea gels (right panels). Mitochondrial proteins were subsequently detected by Western blotting. Preimmune sera, sera and purified antibodies were diluted 1:500, 1:2000 and 1:500, respectively. The calculated molecular masses of *LtTob55*, *LtErv*, *LtsTim1* and *LtTim17* are 52.6, 34.7, 11.6 and 16.3 kDa, respectively. Bands with expected protein sizes are labelled with an asterisk.